JOURNAL OF OPTOELECTRONICS AND ADVANCED MATERIALS Vol. 9, No. 2, February 2007, p. 311 - 314

Solid phase and ion beam epitaxial crystallization of Si implanted with Zn and Pb ions

CH. ANGELOV[*], S. GEORGIEV, B. AMOV, V. MIKLI[a], T. LOHNER[b]
Institute for Nuclear Research and Nuclear Energy, Bulgarian Academy of Sciences, 72 Tzarigradsko Chaussee Blvd., 1784 Sofia, Bulgaria
[a]*Centre for Materials Research, Tallin Technical University, Ehitajate 5, Tallin 79086, Estonia*
[b]*Research Institute for Technical Physics and Materials Science, Konkoly Thege Miklos ut 29-33, H-1121 Budapest, Hungary*

Rutherford backscattering spectroscopy in combination with channelling have been applied to investigate the surface structural changes of silicon implanted with low-soluble species (Zn and Pb) and subsequently thermally and ion beam annealed. For the fast diffusing Zn complete recrystallization during annealing of layers amorphized by ion implantation was observed, while for the slow diffusing Pb incomplete recrystallization took place. The results are discussed with respect to the corresponding experimental conditions.

(Received November 1, 2006; accepted December 21, 2006)

Keywords: Ion implantation, Solid phase epitaxial crystallization, Impurity distribution

1. Introduction

The unique feature of ion implantation is that impurity atoms can be introduced into silicon in concentrations well above the thermal equilibrium solubility value. Precise control and reproducibility of the depth distribution of dopants is required for the fabrication of semiconductor devices. The activation energy for conventional solid phase epitaxial growth (SPEG) in Si has been measured to be around 2.7 eV [1,2]. At the same time, ion beam induced epitaxial crystallization (IBIEC) in Si occurs at temperatures as low as 200-400 ^oC, well below those of the conventional furnace or rapid thermal annealing processes (500-1000 ^oC). The activation energy of such ion induced epitaxy has been measured to be around 0.3 eV, which is one order of magnitude lower than SPEG. It is thus interesting to compare other physical properties between IBIEC and SPEG. Zn is characterized by a fast diffusion coefficient in Si ($D_{Zn}=10^{-7}$-10^{-6} cm^{-2} s^{-1}), while Pb is a very slow diffuser, even in amorphous Si ($D_{Pb}\sim10^{-25}$ cm^{-2} s^{-1}). The impurity elements used in the present study have very low solid solubilities in Si (6×10^{16} cm^{-3} for Zn [3]) and, for the dose used of 1×10^{15} cm^{-2}, the Zn and Pb concentrations greatly exceed the solid solubility limits in Si. Thus it possible to produce non-equilibrium structures with impurities trapped in crystalline Si (c-Si) at such concentrations. Ion implantation of insoluble elements seems to be important in the future fabrication of integrated circuits, and it is also promising for the formation of shallow p-n junctions [4].

In the present work, Rutherford backscattering spectroscopy (RBS) in combination with channeling (RBS/C) has been used to investigate the evolution of the depth profiles of the implanted ions in silicon during IBIEC and SPEG. Spectroscopic ellipsometry (SE) was used for precise measurement of the values of the near-surface amorphization. Reflection high energy electron diffraction (RHEED) and scanning electron microscopy (SEM) were used for structure investigations.

2. Experimental

Czochralski-grown Si (100) wafers, which were p-type, with a resistivity of 17 Ω cm, were amorphized with 100 keV Zn^+ and Pb^+ ions at liquid nitrogen temperature (LNT). In both cases, the implantation dose was 1×10^{15} cm^{-2}, which resulted in peak concentrations of 0.3 at.% for Zn and 0.8 at.% for Pb. Before the SPEG and IBIEC annealing, pre-annealing was performed at 450 ^oC for 1 h in vacuum, to obtain sharp crystalline-amorphous (c-a) interfaces. A thin layer of SiO_2, 4.3 nm for Zn implantation and 5.4 nm for Pb implantation, was formed on the Si surface during this pre-annealing treatment, as measured by a SOPRA ES4G rotating polarizer spectroscopic ellipsometer. These processes resulted in an amorphous layer at the surface with a thickness of 145.1 nm for Zn or 78.6 nm for Pb. A standard tube furnace was used for isothermally annealing in a dry Ar atmosphere for 20, 40 and 60 min at 525 ^oC. Another set of the as-implanted samples was irradiated with 3 MeV Si^+ ions from a 3 MV tandetron in order to stimulate IBIEC. The beam current density was 0.075 μA cm^{-2} and the doses were 5×10^{15}, 1×10^{16} and 2×10^{16} cm^{-2}. The total energy deposition at the depth of the initial c-a interface was 120 eV/atom for the highest dose used, and was nearly constant within the measured depth range. The temperature rise of the irradiated area was negligible and the sample holder temperature was stabilized at 400 ^oC (±2 ^oC).

RBS measurements were performed using a 1.8 MeV He^+ beam from a Van de Graaff accelerator in glancing angle geometry at 100° of the detector to obtain better depth resolution. Some of the Zn implanted and IBIEC annealed samples were investigated in a backward geometry at 165°, to avoid overlapping of the Si and Zn RBS spectra (see Fig. 1). A silicon surface-barrier detector was used with an overall resolution of about 15 keV FWHM. Energy calibrations were performed using 200 Å Au on Si and bulk SiO_2 samples. Complementary information on the nature of the implantation induced structures and surface morphology of the samples was obtained by RHEED and SEM. The measurements were carried out using a TEM-EMV-100B transmission electron microscope working at an accelerating voltage of 100 kV and a Jeol JSM-840A scanning electron microscope. SE measurements were performed using a M-88 rotating analyzer ellipsometer in the wavelength range 280-760 nm, at an angle of incidence of 75.1° for Zn and 70.2° for Pb implanted samples. The depth distributions of both vacancies and implanted atoms were calculated by SRIM-2003 [5].

3. Result and discussion

The implantation and annealing conditions used in this study, and the resulting re-growth thickness of the amorphous Si (a-Si) and SiO_2, due to the thermal annealing, are summarized in Table 1.

Table 1. Summary of the implantation conditions and the SE results for the thickness of a-Si and SiO_2 layers of SPEG samples, obtained in the present work.

Projectile ion 100 keV, 1×10^{15} cm^{-2}		Thickness of a-Si and SiO_2 (nm)			
		as-implanted	20 min	40 min	60 min
Zn	SiO_2 a-Si	4.3 145.1	4.2 73.1	4.2 1.7	4.2 1.2
Pb	SiO_2 a-Si	5.4 78.6	5.4 41.0	5.4 26.0	4.2 20.2

After ion implantation with a dose of 1×10^{15} cm^{-2} and energy of 100 keV, no reflections were present in the RHEED pattern for Zn and for Pb, indicating that complete surface amorphization of the Si wafer had taken place. The surface morphology of the as-implanted samples was revealed by SEM. No structural features can be seen for as-implanted with Zn and Pb samples, at a dose of 1×10^{15} cm^{-2}. The SPEG and IBIEC annealing did not lead to any apparent changes in the surface morphology. Fig. 1 shows random (a) and channeling (b) spectra of samples implanted with Zn, before and after SPEG annealing for various times. The amorphous layer initially formed was 145.1 nm with 4.3 nm SiO_2 on the Si surface (Table 1). The regrowth thickness increased with increasing annealing time, and almost complete recrystallization took place for the annealing time of 40 min. The mean re-growth rate was 3.6 nm/min. During SPEG annealing, the zink impurity peak shifted to the surface. This shift and the decrease of the width of the peak are attributed to outdiffusion of the Zn atoms. The height of Zn peak reached a maximum in the case of 40 min annealing (Fig. 1 (a)). Most of the Zn atoms (~65%) are in a substitutional sites. Increasing the annealing time to 60 min led to small decrease of a-Si layer (Table 1). A backward diffusion of the Zn atoms occurred, occupying ~82 % substitutional sites (Fig. 1, aligned yield/random yield). The crystallization process after SPEG of Pb-implanted Si (Fig. 2) was different. The initially formed amorphous layer was 78.6 nm with 5.4 nm SiO_2 on the Si surface (Table 1). The regrowth thickness increased with increasing the annealing time. Even for the highest annealing time (60 min) incomplete recrystallization was observed (Table 1, Fig. 2 (b)). The mean re-growth rate decreased from 1.8 nm/min for the first part of the annealing to 0.3 nm/min for highest annealing time. Redistribution of the initially formed Pb profile in a-Si occurred when the c-a interface passed through it under SPEG. A double Pb peak in the near-surface region was detected for the final annealing step. The substitutional Pb in the recrystallized part of the Si layer was about 86 %.

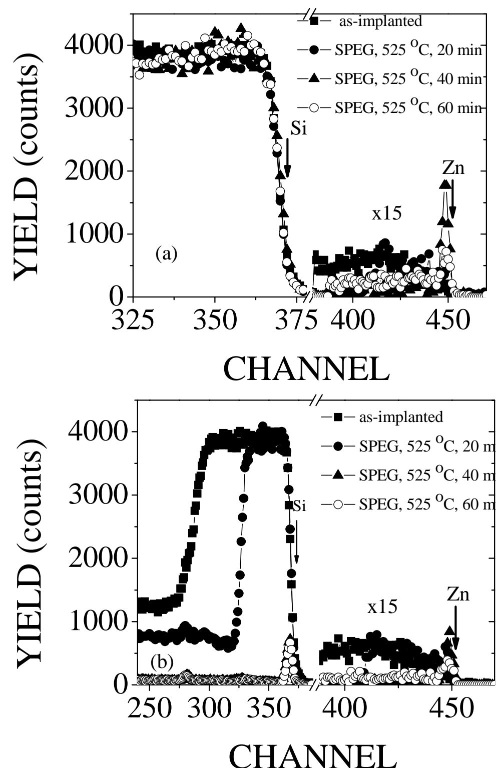

Fig. 1. RBS random (a) and aligned spectra (b) of Zn^+ implanted Si with a dose of 1×10^{15} cm^{-2} at a glancing angle (100°).

The implantation and annealing conditions used in our study and the resulting re-growth thickness of a-Si and SiO_2 resulting from the ion beam annealing are summarized in Table 2.

Fig. 3 (a) shows the channeling spectra of Si samples implanted with Zn before and after irradiation at 3 MeV Si^+ beam at various annealing doses. The re-growth thickness increased with increasing annealing dose from 5×10^{15} cm^{-2} to 2×10^{16} cm^{-2}. The highest annealing dose was sufficient for almost complete recrystallization of the amorphised Si layer. As in the case of SPEG, the out-diffusion of Zn took place during IBIEC.

For the highest annealing dose of 2×10^{16} cm^{-2}, the retained amount of Zn atoms in the Si substrate was only a few percent, compared to the respective implanted dose of Zn which was measured to be 1×10^{15} cm^{-2}. It suggests that massive diffusion, accompanied by strong liberation of Zn from the near-surface region occurred during the IBIEC.

The crystallization process after IBIEC of Pb-implanted Si (Fig. 3 (b)) was different. For the highest dose of annealing (2×10^{16} cm^{-2}) incomplete recrystallization was observed (Table 2). The out-diffusion of Pb atoms in a-Si occurred when the c-a interface passed through it under IBIEC.

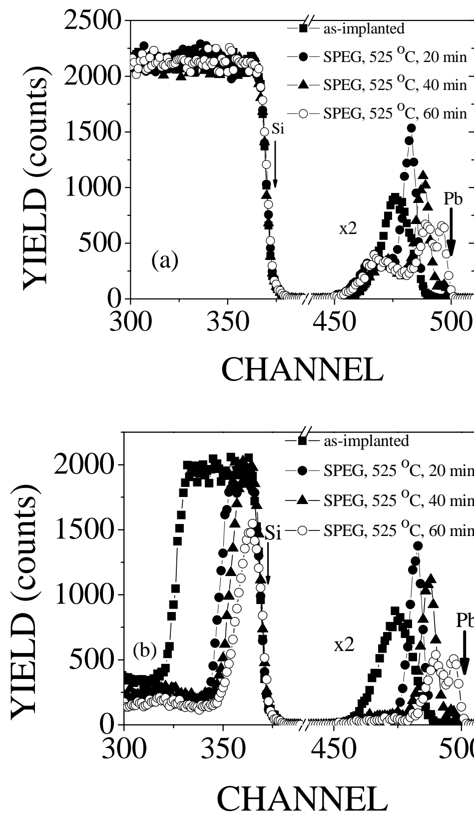

Fig. 2. RBS random (a) and aligned spectra (b) of Pb^+ implanted Si with a dose of $1x10^{15}$ cm^{-2} at a glancing angle (100°).

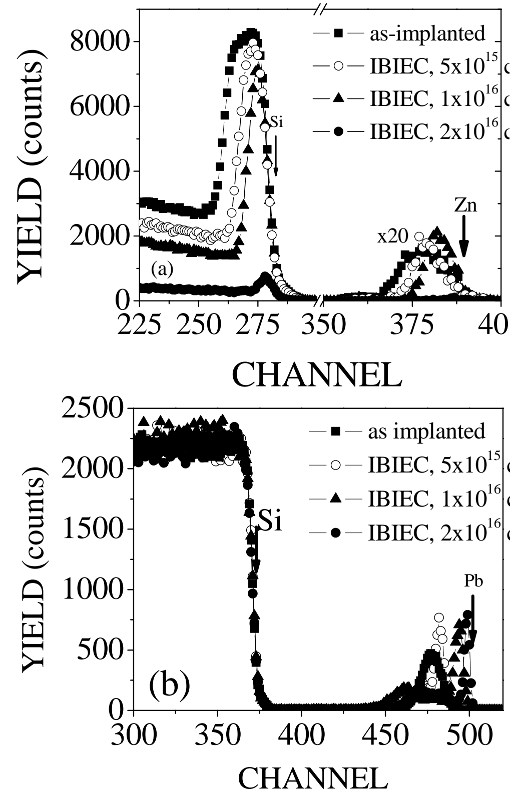

Fig. 3. RBS spectra of Zn^+ at a backscattering angle of 165° in a channeling condition (a) and Pb^+ (b) implanted Si at a glancing angle 100°, for a random orientation after IBIEC.

Table 2. Summary of the implantation conditions and the SE results for the thickness of a-Si and SiO_2 layers of IBIEC samples, ($1 - 5\times10^{15}$ cm^{-2}, $2 - 1\times10^{16}$ cm^{-2}, $3 - 2\times10^{16}$ cm^{-2}).

Projectile ion 100 keV, 1×10^{15} cm^{-2}		Thickness of a-Si and SiO_2 (nm)			
		as-impl.	1	2	3
Zn	SiO_2	4.3	4.6	5.8	6.4
	a-Si	145.1	75.6	56.6	0.9
Pb	SiO_2	5.4	6.1	5.1	6.4
	a-Si	78.6	35.4	10.7	1.7

During the time of the second annealing dose (1×10^{16} cm^{-2}) of the IBIEC processing (20000 s), the substitutional part of the implanted Pb species reached saturation (~62%). After this some of the substitutional Pb escaped to interstitial positions. With the help of Si-interstitials, these species diffused during the remaining the time (more than 20000 s) for the highest dose of IBIEC (2×10^{16} cm^{-2}). This result is consistent with the model proposed by Cho et al. [6].

In attempting to explain these observations, it should be noted that SPEG was performed at 525 °C and IBIEC was performed at 400 °C during irradiation. The melting points of these species are $T_{m,Zn}$ = 419.5 °C and $T_{m,Pb}$ = 327.6 °C.

The most plausible explanation of the Zn and Pb push-out effects under SPEG and IBIEC is a melt-mediated crystallization process occurring during annealing. Zn atoms diffuse rapidly Si, and are able to escape from the c-a boundary as it moves to the surface. The presence of slow diffusing Pb in a-Si inhibits the crystallization processes at temperature 525 ^{o}C.

According to Fig. 3(b), it appears that in the case of Pb implantation, the phase transformation in the a-Si layer during IBIEC is controlled by transient enhanced diffusion [7] as well.

4. Conclusion

The evolution of Zn and Pb species, implanted in Si during the pure thermal and ion beam induced crystallization of the amorphized substrates has been analyzed using RBS, SE, RHEED and SEM. Massive redistribution of the initially formed profiles of Zn and Pb was observed during the annealing. In the case of SPEG, the impurity atoms with low solubility and high diffusivity (Zn) could escape to the surface with the c-a interface, as shown in Fig. 1.

The impurities with low diffusivity (Pb) could not follow the moving c-a interface. As a result, they were "frozen" in the crystalline phase after the c-a interface passed through, resulting in a higher impurity concentration than the normal solid solubility (i.e. supersaturation). The present results indicated that IBIEC also achieves the supersaturation of impurity atoms, but the impurity substitution is less than that for SPEG. The results of this study clearly show the possibility of the formation of structures with high volume concentrations of insoluble dopants in a non-equilibrium way.

References

[1] R. G. Elliman, J. S. Williams, R. V. Knoel, Nucl. Instr. and Meth. B **19-20**, 435 (1987).
[2] F. Priolo, Mat. Sci. Rep. **5**, 319 (1990).
[3] A. J. Milnes, Deep Impurities in Semiconductors (Wiley, New York; Russian edition, Mir, M., 1977), p. 38.
[4] Y. Ishikawa, I. Kobayashi, I. Nakamichi, Jpn. J. Appl. Phys. **29,** 1929 (1990).
[5] J. Ziegler, The Stopping and Range of Ions in Solids, New York, Pergamon Press, (1986).
[6] K. Cho, M. Numan, T. G. Finstad, W. K. Chu, J. Liu, Appl. Phys. Lett. **47**, 1321 (1985).
[7] S. C. Jain W. Schoenmaker, Decoutere, M. Willander, J. Appl. Phys. **91**, 8919 (2002).

*Corresponding author: changelov@inrne.bas.bg